Activity differentially regulates the surface expression of synaptic AMPA and NMDA glutamate receptors

Dmitri V. Lissin*, Stephen N. Gomperts†, Reed C. Carroll*, Chadwick W. Christine‡, Daniel Kalman§, Marina Kitamura¶, Stephen Hardy¶, Roger A. Nicoll‖,**, Robert C. Malenka*,‖,††, and Mark von Zastrow*,**

Departments of *Psychiatry, ‖Physiology, ‡Neurology, **Cellular and Molecular Pharmacology, and §Microbiology and Immunology, and †Graduate Program in Neuroscience, University of California, San Francisco, CA 94143; and ¶Cell Genesys Inc., Foster City, CA 94404

ABSTRACT   Distinct subtypes of glutamate receptors often are colocalized at individual excitatory synapses in the mammalian brain yet appear to subserve distinct functions. To address whether neuronal activity may differentially regulate the surface expression at synapses of two specific subtypes of ionotropic glutamate receptors we epitope-tagged an AMPA (α-amino-3-hydroxy-5-methylisoxazole-4-propionic acid) receptor subunit (GluR1) and an NMDA (*N*-methyl-D-aspartate) receptor subunit (NR1) on their extracellular termini and expressed these proteins in cultured hippocampal neurons using recombinant adenoviruses. Both receptor subtypes were appropriately targeted to the synaptic plasma membrane as defined by colocalization with the synaptic vesicle protein synaptophysin. Increasing activity in the network of cultured cells by prolonged blockade of inhibitory synapses with the γ-aminobutyric acid type A receptor antagonist picrotoxin caused an activity-dependent and NMDA receptor-dependent decrease in surface expression of GluR1, but not NR1, at synapses. Consistent with this observation identical treatment of noninfected cultures decreased the contribution of endogenous AMPA receptors to synaptic currents relative to endogenous NMDA receptors. These results indicate that neuronal activity can differentially regulate the surface expression of AMPA and NMDA receptors at individual synapses.

Information about the mechanisms of synaptic transmission and synaptic plasticity in the mammalian brain derives primarily from electrophysiological studies of excitatory synapses in the hippocampus. These synapses use the neurotransmitter glutamate, which can act on distinct subtypes of ionotropic and metabotropic receptors that frequently colocalize at individual synapses but appear to subserve distinct functions (1–3). Two major subtypes of ionotropic receptors, AMPA (α-amino-3-hydroxy-5-methylisoxazole-4-propionic acid) and NMDA (*N*-methyl-D-aspartate) receptors, have been found at virtually all excitatory synaptic connections in the mammalian brain. AMPA receptors (AMPARs) are heteromers of the homologous subunits GluR1–4 and mediate the bulk of synaptic transmission during basal neural activity (1–3). NMDA receptors (NMDARs) also exist as heteromers formed from the NR1 subunit and one or more NR2A-D subunits (1–3). Because of their voltage dependence and high calcium permeability, NMDARs are particularly important for triggering several different forms of synaptic plasticity, including long-term potentiation and long-term depression. When inappropriately activated during a variety of pathological conditions, NMDARs also contribute to neuronal injury and death.

It has commonly been assumed that AMPARs and NMDARs are colocalized at individual synapses (1–4), although it is now clear that these receptor subtypes interact with different proteins at the synapse (5). The distinct molecular interactions and functions of these receptor subtypes raise the possibility that their surface expression at synapses may be independently regulated. Consistent with this idea, recent electrophysiological data on the mechanisms of long-term potentiation have suggested that a proportion of synapses in the hippocampus may be functionally silent because NMDARs, but not AMPARs, are present in the postsynaptic membrane (6–8). Thus during periods of low activity when the membrane potential remains relatively hyperpolarized, glutamate release fails to generate a postsynaptic response. After long-term potentiation, however, these synapses appear to become functional, perhaps because AMPARs are inserted into the membrane. Similar results also have been obtained in the frog optic tectum (9) and thalamocortical synapses in somatosensory cortex (10), suggesting that the independent regulation of the surface expression of AMPARs and NMDARs may be a ubiquitous property of excitatory synapses. However, alternative hypotheses that do not require differential regulation of AMPARs and NMDARs have been proposed to account for these data (11).

A more direct approach to the question of whether the expression of AMPARs and NMDARs in the postsynaptic membrane may be independently regulated by activity involves the direct visualization of receptors located on the cell surface by using immunofluorescence techniques. Because there are intracellular pools of glutamate receptors (12–15), visualization of only those receptors inserted in the plasma membrane requires the use of antibodies that bind to epitopes on the extracellular domain of the receptor under conditions that preserve membrane integrity. To accomplish this, we have epitope-tagged the extracellular (N terminus) domains of the AMPAR subunit GluR1 and the NMDAR subunit NR1 and expressed these proteins in hippocampal cells in culture by using recombinant adenoviruses. We then examined the effects of manipulating neuronal activity on the surface expression of these receptor subtypes.

METHODS

Epitope Tagging and Expression in HEK293 Cells. The cDNA encoding rat GluR1 (flop) (clone provided by S. Heinemann, Salk Institute, San Diego) was epitope-tagged at the amino

Abbreviations: AMPA, α-amino-3-hydroxy-5-methylisoxazole-4-propionic acid; NMDA, *N*-methyl-D-aspartate; AMPAR, AMPA receptor; NMDAR, NMDA receptor; EPSC, excitatory postsynaptic current; HA, hemagglutinin; APV, 2-amino-5-phosphonovaleric acid; mEPSC, miniature EPSC.
††To whom reprint requests should be addressed at: Department of Psychiatry, University of California, LPPI, Box 0984, 401 Parnassus Avenue, San Francisco, CA 94143. e-mail: malenka@itsa.ucsf.edu.

terminus by using a shuttle vector containing a 5′ cleavable signal sequence followed by a Flag epitope tag sequence (DYKD-DDDK). Similarly NR1 (clone provided by P. Seeburg, Max-Planck-Institute, Heidelberg) was epitope-tagged at the amino terminus with a signal sequence followed by a hemagglutinin (HA) epitope tag (YPYDVPDYA). Constructs were subcloned into pcDNA3 (Invitrogen) for HEK293 transfections. HEK293 cells were transfected with either Flag-GluR1 or HA-NR1 and NR2B along with pcDNA3-GFP to visualize transfected cells. Cells were transfected by using Lipofectamine (GIBCO) 48 hr before recording. Whole-cell recordings were made by using an Axopatch 1D. Flag-GluR1 expressing cells were maintained at room temperature in 115 mM NaCl, 5.4 mM KCl, 1.8 mM $CaCl_2$, 0.78 mM $MgCl_2$, 5 mM Hepes, 23 mM glucose, 26 mM sucrose with 50 μM cyclothiazide. HA-NR1 expressing cells were recorded in a similar saline lacking Mg^{2+} and containing 20 μM glycine. The pipette solution contained 115 mM K-gluconate, 5 mM NaCl, 5 mM NaHepes, 5 mM EGTA, 1.48 mM $CaCl_2$, 0.67 mM $MgCl_2$, 1.5 mM MgATP, 0.1 mM MgGTP. Cells were held at -70 mV in voltage clamp. Glutamate (300 μM) was applied to cells for 200 ms via perfusion pipettes controlled by solenoid valves. Application of glutamate to untransfected cells yielded no response ($n = 6$).

Hippocampal Cultures. Hippocampi of postnatal day 0 Sprague–Dawley rat pups were removed, and the dentate gyri were grossly dissected and discarded. Cells derived from the remaining tissue were plated as described in Lester *et al.* (16) except that papain was not used. B27-supplemented neurobasal cultures were prepared as described in Brewer *et al.* (17), and 50 units/ml of both streptomycin and penicillin were added. One-half of the growth medium was exchanged 1 day after plating and weekly thereafter.

Adenovirus Construction and Expression in Hippocampal Neurons. Epitope-tagged GluR1 and NR1 were subcloned into a plasmid vector containing a tetracycline repressor binding sequence upstream of the transcriptional start site and viral recombination sites. Recombinant viruses encoding engineered receptor constructs were produced by using a Cre-lox recombination system as described in Hardy *et al.* (18). Day 12 hippocampal cultures were exposed for 30 min to virus (at a multiplicity of infection of 10^7 particles per ml) expressing Flag-GluR1 or HA-NR1 together with a virus constitutively expressing tetracycline repressor-VP16 fusion protein, which was required to activate expression of Flag-GluR1 or HA-NR1. Cells then were washed, reincubated in the previously removed media, and after 48 hr, assayed for expression of the receptors.

Immunocytochemistry. Cells were fixed in 4% paraformaldehyde in PBS and permeabilized with 0.1% Triton X-100 in PBS. The mouse mAbs anti-Flag M1 (Kodak) and anti-HA 12CA5 (Boehringer Mannheim) were applied for 1 hr to stain the Flag and HA epitopes, respectively. Receptor immunoreactivity was visualized by secondary antibody staining by using goat anti-mouse IgG conjugated to Cy3 (Jackson ImmunoResearch). For staining under nonpermeabilizing conditions, cells were fixed with 4% paraformaldehyde in PBS and exposed to M1 or 12CA5 for 1 hr. After washing, a secondary goat anti-mouse horseradish peroxidase conjugate was applied, and receptor immunoreactivity was detected by using tyramide signal amplification (TSA-Direct, NEN). Identical images were obtained (i.e., punctate clusters of Flag-GluR1 or HA-NR1) when primary antibodies (M1, 12CA5) were applied to living cells and washed out before fixation. Cells not exposed to virus and processed identically to infected cells did not stain with M1, 12CA5, or anti-mouse secondary antibodies under permeabilized or nonpermeabilized processing conditions. To stain for synaptophysin, cells were permeabilized with 0.1% Triton X-100 and incubated with rabbit anti-synaptophysin antiserum (Zymed) followed by goat anti-rabbit IgG Cy3 conjugate. Identification of glutamate receptor clusters and

their colocalization with synaptophysin was accomplished with dual color microscopy using a Nikon 60× objective (NA1.4) and standard fluorescein and Cy3 filter sets (Omega). Microscopic fields (200 μm × 300 μm) were visualized from blindly coded coverslips, and fields containing both transfected neurons and numerous synaptic contacts (identified by synaptophysin immunoreactivity) were chosen randomly for acquisition. Fluorescent images were acquired by using a cooled digital charge-coupled device camera (Princeton Instruments, Trenton, NJ). Images were analyzed by using IPLab analysis software and displayed as dual-color merged images by using Adobe Photoshop. Cultures not expressing recombinant receptors were stained and imaged in the same manner to define background levels of fluorescence. Staining uninfected cells for synaptophysin revealed no fluorescent Cy3 puncta when viewed in the fluorescein channel. Synaptic structures (identified as synaptophysin-positive puncta) were scored as receptor-positive if the intensity of receptor immunoreactivity was >2-fold higher than the background level. Most receptor-positive synaptic structures had fluorescence intensities >4-fold higher than background. For all experiments, control and picrotoxin-treated cultures were from the same preparation and were processed for immunofluorescence in parallel. All data acquisition and analysis were performed blindly, without knowledge of the treatment to which the culture dish had been exposed. For all immunocytochemical experiments, *n* refers to the number of fields analyzed. Three to five fields were examined per culture dish. GAD65 was visualized by immunostaining using a specific mouse mAb (GAD6, provided by S. Baekkeskov, University of California, San Francisco). Localization of GAD65 (labeled by Cy3-conjugated secondary antibody) to synaptic structures was determined by costaining with rabbit antisynaptophysin (labeled by fluorescein isothiocyanate-conjugated secondary antibody). Dual-color images were blindly acquired from 20 fields for each condition, and analysis of GAD65-positive synaptic structures was performed as above on the digital images.

Electrophysiology in Cultured Hippocampal Neurons. Cultures were prepared and treated exactly as for the immunocytochemistry experiments but were not exposed to adenovirus. Paired whole-cell recordings were made at room temperature from 11- to 15-day-old picrotoxin-treated and control neurons with two Axopatch-1D amplifiers using low resistance patch pipettes (2–5 MΩ). Pipette solutions contained: 122.5 mM Cs-gluconate, 8 mM NaCl, 10 mM Hepes, 0.2 mM EGTA, 2 mM MgATP, 0.3 mM NaGTP, adjusted to pH 7.4 with CsOH. The extracellular solution contained: 140 mM NaCl, 3.5 mM KCl, 10 mM Hepes, 20 mM glucose, 0.5–0.75 mM $CaCl_2$, 7 mM $MgCl_2$, 20 μM glycine, and 50 μM picrotoxin adjusted to pH 7.3 with NaOH. Mg^{2+} was increased and Ca^{2+} decreased to minimize any possible polysynaptic contamination of the monosynaptic currents. When recording evoked excitatory postsynaptic currents (EPSCs), postsynaptic cells were held at $+40$ to $+60$ mV. Presynaptic cells were held at -60 mV and were stimulated once every 10–20 sec with a 2.5 msec to 20 msec depolarizing current pulse. AMPAR-mediated currents were isolated by the addition of 50 μM D-2-amino-5-phosphonovaleric acid (APV) (Tocris Neuramin, Bristol, U.K.); NMDAR-mediated currents were isolated by the addition of 5 μM NBQX (2–3-dihydroxy-6-nitro-7-sulfamoylbenzo[*f*]quinoxaline; Tocris Neuramin). Synaptic currents were completely abolished with addition of both D-APV and NBQX. Series resistance compensation (80%) was used in all experiments. The series and input resistances were monitored throughout each experiment with a -6 mV calibration pulse given 25–40 msec before each stimulation. Evoked EPSCs were acquired and analyzed on-line by using custom software developed by D. Selig (University of California, San Francisco). Currents were low-pass filtered at 2 kHz

and digitally sampled at 5 kHz. AMPAR and NMDAR EPSC peak amplitudes were measured from the average of 8–16 traces. For recording miniature EPSCs (mEPSCs), cells were held at -60 mV in extracellular solution containing: 3 mM Ca^{2+}, 2 mM Mg^{2+}, 1 μM tetrodotoxin, 50 μM picrotoxin, and 50 μM D-APV. mEPSCs were acquired by using Axoscope (Axon Instruments) and were analyzed by using Mini™ (J. Steinbach, Washington University, St. Louis). Threshold mEPSC amplitude was set at 5 pA, and 100–900 events were collected and averaged to calculate the mean mEPSC amplitude for each culture preparation examined.

Western Blot Analysis. Transfected cells from hippocampal cultures were lifted with cold PBS, pelleted, and resuspended in warm SDS sample buffer (New England Biolabs). After SDS/PAGE and blotting onto nitrocellulose, paired lanes of control and 2-week picrotoxin-treated samples were probed with anti-Flag M1 antibodies (Kodak). Untransfected cultures were prepared similarly and probed with antibodies to GluR1 (provided by R. Huganir, Johns Hopkins University, Baltimore; ref. 15) or GluR2/3 (Chemicon). Horseradish peroxidase-conjugated secondary goat anti-rabbit or anti-mouse antisera were used followed by chemiluminescence detection (ECL; Amersham), and blots were digitally scanned from x-ray film.

RESULTS

Using standard recombinant techniques we initially epitope-tagged the extracellular (N terminus) domains of GluR1 and NR1 with Flag and HA epitopes, respectively (called Flag-GluR1 and HA-NR1) (Fig. 1*A*). Application of glutamate to HEK293 cells transfected with cDNAs encoding Flag-GluR1 or HA-NR1 (and NR2B) generated inward currents that were blocked by the appropriate subtype-specific antagonist (Fig. 1*A*; $n = 4$ for GluR1 and $n = 5$ for NR1). Thus the epitope tag did not impair the electrophysiological function of these channels.

To determine whether Flag-GluR1 and HA-NR1 are localized to synapses we next expressed them, using recombinant adenoviruses, in primary hippocampal neurons in culture. Staining permeabilized cells revealed that 2 days after infection, most neurons and glia ($>70\%$) expressed readily detectable levels of epitope-tagged receptors that were diffusely distributed throughout the soma and dendrites (Fig. 1*B*) and were localized primarily in intracellular membranes. When stained under nonpermeabilized conditions only receptors in the plasma membrane were observed, revealing punctate clusters of Flag-GluR1 or HA-NR1 in neurons (Fig. 1*C*) but not in glia (as differentiated by costaining for neuron-specific enolase; not shown). Importantly, these surface clusters of
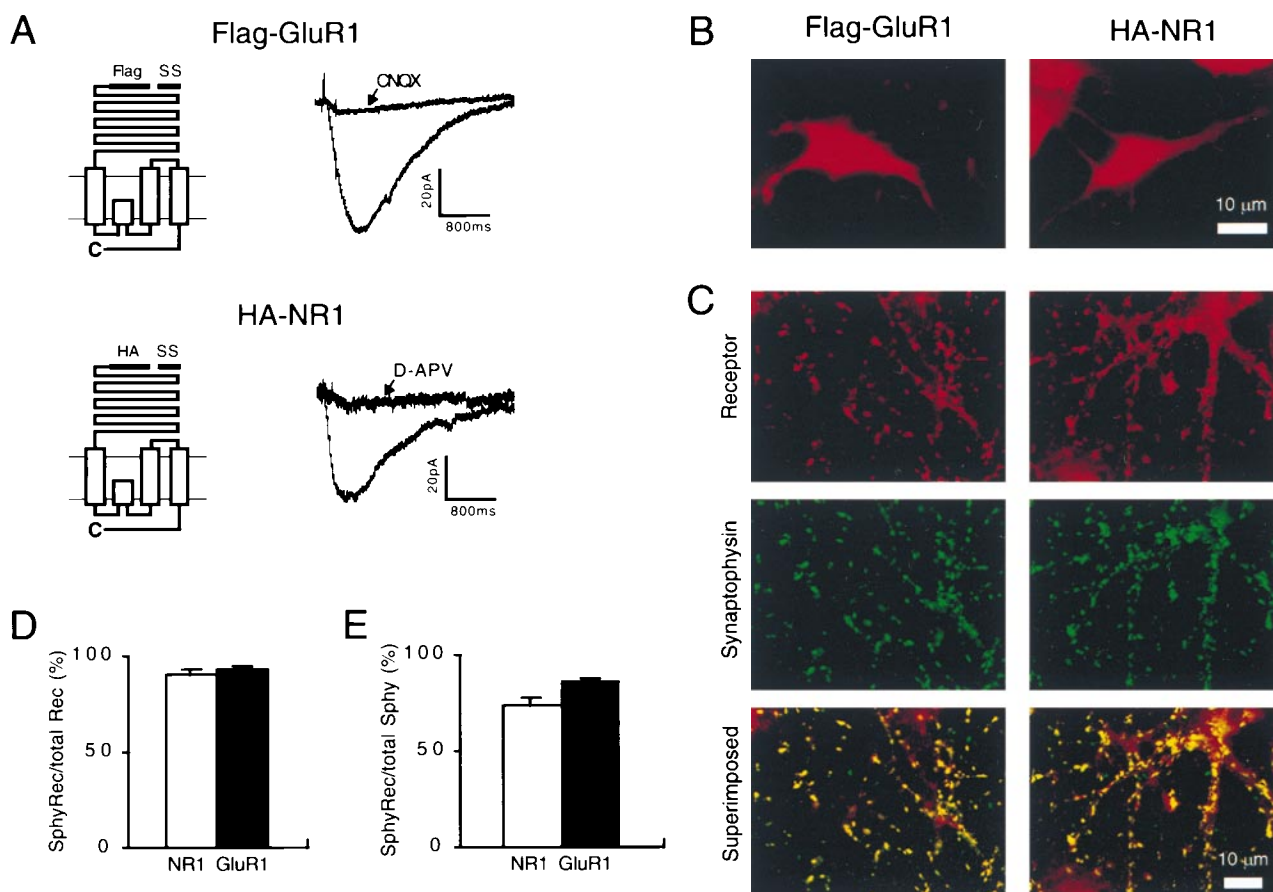

FIG. 1. Epitope-tagged GluR1 and NR1 form functional channels and are targeted to synaptic membranes. (*A*) (*Left*) Diagram of the epitope-tagged GluR1 (*Upper*) and NR1 (*Lower*). SS, signal sequence. (*Right*) The inward currents generated by application of glutamate to HEK293 cells expressing Flag-GluR1 (*Upper*) or HA-NR1 with NR2B (*Lower*). The currents are blocked by the appropriate subtype-specific antagonist. (*B*) Examples of the receptor distribution that is observed when hippocampal neurons expressing Flag-GluR1 or HA-NR1 are permeabilized before applying the primary receptor antibodies. (*C*) (*Top*) Typical receptor distributions when neurons are not permeabilized and stained for Flag-GluR1 or HA-NR1. (*Middle*) The distribution of synaptophysin puncta in the same fields. (*Bottom*) The superimposed images illustrate that the vast majority of Flag-GluR1 and HA-NR1 clusters colocalize with synaptophysin. (*D*) Quantitation of the percentage of Flag-GluR1 and HA-NR1 clusters that colocalize with synaptophysin ($n = 20$ for each subtype) indicates that the vast majority of Flag-GluR1 and HA-NR1 clusters are at synapses. (*E*) Quantitation of the percentage of synaptophysin puncta that colocalize with Flag-GluR1 and HA-NR1 ($n = 20$ for each subtype) indicate that the majority of synapses are excitatory and contain epitope-tagged receptors. The remaining synapses presumably are inhibitory because 10–30% of synaptophysin puncta colocalized with GAD65 (see Fig. 2*D*). Error bars represent SEM.

epitope-tagged GluR1 or NR1 colocalized with the presynaptic protein synaptophysin (Fig. 1C). Quantitation of this colocalization (Fig. 1D) demonstrated that approximately 90% of the Flag-GluR1 and HA-NR1 surface receptor clusters were localized at synapses ($n = 20$). Of the total number of synapses in the cultures, the vast majority expressed Flag-GluR1 and HA-NR1 (Fig. 1E). The remaining synapses were likely to be inhibitory because approximately 20% of the synaptophysin puncta colocalized with the γ-aminobutyric acid synthetic enzyme, GAD65 ($n = 20$).

Having established that Flag-GluR1 and HA-NR1 are targeted to synapses and expressed in the postsynaptic membrane, we next wanted to determine whether targeting was affected by alterations in the level of activity. We therefore treated cultures with the γ-aminobutyric acid type A receptor antagonist picrotoxin, an agent that blocks inhibitory synaptic transmission in the network of cultured neurons and consequently increases network activity. Control and picrotoxin-treated cultures were infected with recombinant adenoviruses expressing Flag-GluR1 or HA-NR1 after 12 days of picrotoxin treatment. Two days later, the localization of receptors to synaptic membranes was examined. Examples of the effect of picrotoxin on the targeting of Flag-GluR1 and HA-NR1 are shown in Fig. 2A, and a summary of these experiments ($n = 20$) is shown in Fig. 2B. Picrotoxin treatment had no discernible effect on the surface expression of HA-NR1 at synapses. Surprisingly, however, the same treatment caused a significant

decrease in the surface expression of Flag-GluR1 such that only 50% of synapses contained surface GluR1 clusters as compared with 86% of synapses in the sister control cultures. This effect of picrotoxin on the surface expression of GluR1 appeared highly specific. The total number of synapses was the same in control and picrotoxin-treated cultures (Fig. 2C) as was the percentage of inhibitory synapses (Fig. 2D). As in the control cultures, 90% of the Flag-GluR1 clusters in the picrotoxin-treated cultures were at synapses (Fig. 2E), indicating that the clusters did not diffuse laterally in the membrane away from the synapse. It is unlikely that the picrotoxin treatment reduced mRNA expression of Flag-GluR1 because Flag-GluR1 and HA-NR1 expression were identically controlled by a cytomegalovirus promoter. Furthermore, measurement of the level of expression of Flag-GluR1 by Western blotting of culture extracts revealed no effect of the picrotoxin treatment (Fig. 2F). A limitation of this measurement of Flag-GluR1 expression is that glia, as well as neurons, take up adenovirus and express Flag-GluR1. We therefore also measured total Flag-GluR1 immunoreactivity in permeabilized neurons, and again this measure revealed no difference between picrotoxin-treated and control cells (Fig. 2G).

Is the selective effect of picrotoxin on synaptic targeting of Flag-GluR1 indeed caused by activity? To test this we examined the effect of tetrodotoxin (TTX), a toxin that blocks neural activity by blocking voltage-dependent sodium channels. Fig. 3A shows that picrotoxin caused a significant de-
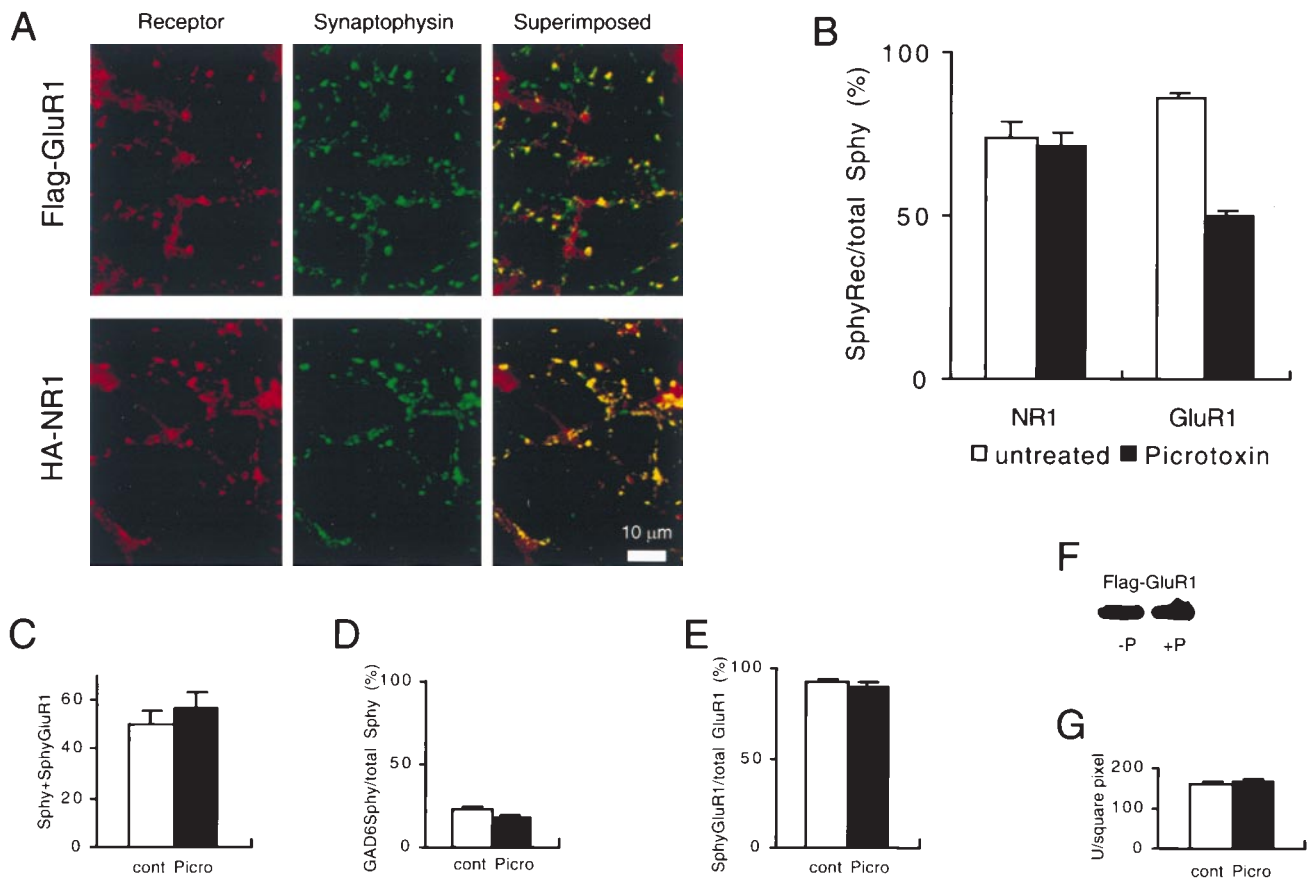

FIG. 2. Increasing activity causes a decrease in synaptic membrane clusters of Flag-GluR1 but not HA-NR1. (A) Example of the staining patterns that are observed after treatment with picrotoxin. Note that many of the synaptophysin puncta do not colocalize with Flag-GluR1. (B) Quantitation of the percentage of synaptophysin puncta that colocalize with Flag-GluR1 or HA-NR1 in untreated and picrotoxin-treated cultures. Picrotoxin had no effect on HA-NR1 but caused a significant reduction in the synaptic localization of surface clusters of Flag-GluR1 ($n = 20$ for each condition). (C) The average number of synapses per microscopic field, as defined by synaptophysin staining, was not affected by picrotoxin treatment. (D) The percentage of inhibitory synapses, as measured by GAD65 staining, was not affected by picrotoxin treatment. (E) The percentage of Flag-GluR1 clusters that colocalize with synaptophysin was not affected by picrotoxin treatment. (F) Western blot showing that picrotoxin treatment did not change the level of expression of Flag-GluR1. (G) Total Flag-GluR1 immunoreactivity in the somas of permeabilized cells was not affected by picrotoxin treatment, as measured by integration of total receptor immunoreactivity using NIH Image software. Error bars represent SEM.
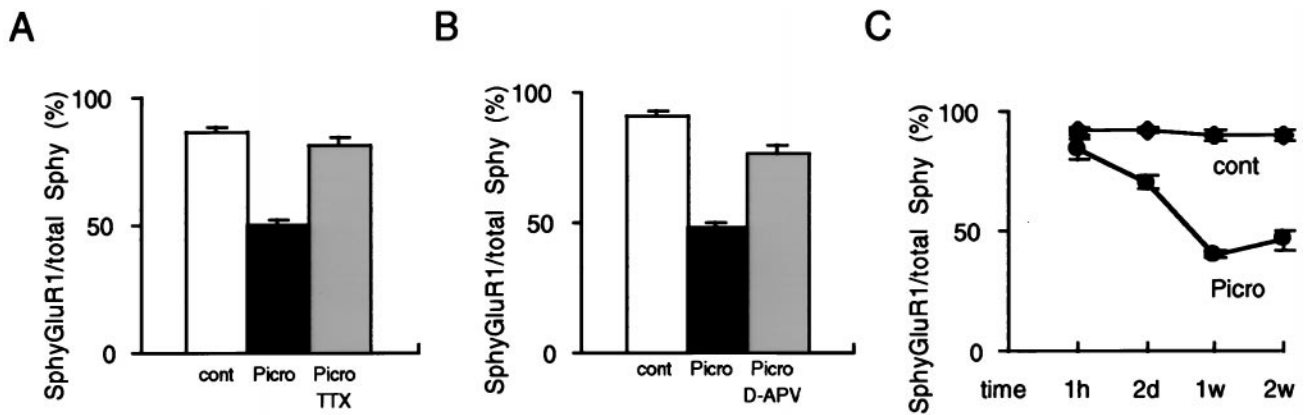
FIG. 3.   The decrease in the surface expression of Flag-GluR1 clusters at synapses is activity- and time-dependent. The Na^+ channel toxin tetrodotoxin (*A*) or the NMDAR antagonist D-APV (*B*) largely prevented the picrotoxin-induced decrease in the proportion of synapses containing surface clusters of Flag-GluR1. Each graph illustrates the percentage of synaptophysin puncta that colocalize with Flag-GluR1. (*C*) The time course of the picrotoxin-induced effect. The abcissa shows the duration of picrotoxin treatment. Error bars represent SEM.

crease in the targeting of Flag-GluR1 to synaptic membranes, and that this effect was completely abrogated by concomitant application of TTX. Because of the importance of NMDARs in triggering synaptic plasticity we next examined the effects of the NMDAR antagonist D-APV on the picrotoxin-induced changes. D-APV also largely prevented the picrotoxin-induced decrease in surface Flag-GluR1 clusters at the synapse (Fig. 3*B*). Thus the targeting of Flag-GluR1 to synaptic membranes appears to be regulated by activity and, at least in part, is under the control of NMDARs. In another series of experiments we examined the time course of the decrease in the Flag-GluR1 synaptic membrane clusters. A clear decrease in the proportion of synapses expressing surface Flag-GluR1 clusters was observed after 2 days of picrotoxin treatment but not after 1 hr (Fig. 3*C*). Maximum effects were seen after 1 week of treatment.

In a final set of experiments we attempted to address two important and related questions. Does picrotoxin treatment cause the same decrease in endogenous synaptic AMPARs,
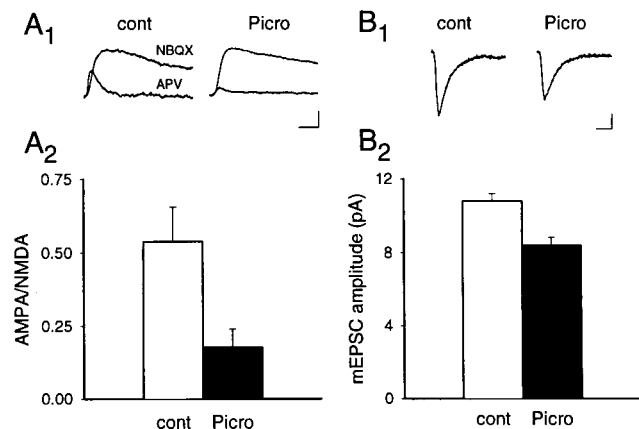

FIG. 4.   AMPAR-mediated synaptic currents are decreased by picrotoxin treatment. (*A*) The ratio of AMPAR- to NMDAR-mediated synaptic currents is decreased in picrotoxin-treated cultures. Examples of the EPSCs (*A1*) recorded from untreated and picrotoxin-treated cultures and (*A2*) a summary ($n = 5$ for untreated cells; $n = 6$ for picrotoxin-treated group) of the AMPAR-to-NMDAR EPSC ratios obtained from each group. Note that the NMDAR EPSCs were scaled for ease of comparison. [Scale bar represents 25 msec and 15 pA (untreated) or 50 pA (picrotoxin).] (*B*) The amplitude of mEPSCs is decreased in picrotoxin-treated cultures. Examples of mEPSCs (average of 200–400) (*B1*) and a summary of all recordings (*B2*) ($n = 6$ for control cultures; $n = 5$ for picrotoxin-treated cultures). (Scale bar represents 10 msec and 2 pA.) Error bars represent SEM.

but not NMDARs, and does this change in the synaptic distribution of surface receptors have clear functional consequences? To answer these questions we treated uninfected cultures with picrotoxin and compared the synaptic currents generated by AMPARs and NMDARs with those recorded from sister control cultures. Fig. 4*A* shows that the ratio of the AMPAR-mediated EPSC to the NMDAR-mediated EPSC was significantly reduced in the picrotoxin-treated cultures. The magnitude of this reduction (67%; control cells ratio, 0.54 ± 0.1, $n = 5$; treated cells ratio, 0.18 ± 0.01, $n = 6$) was similar to the magnitude of the reduction in the percentage of synapses expressing epitope-tagged GluR1. Picrotoxin treatment also significantly decreased the amplitude of AMPAR-mediated mEPSCs (Fig. 4*B*) (mEPSC amplitude in control cultures: 10.8 ± 0.4 pA, $n = 6$; in picrotoxin-treated cultures: 8.4 ± 0.4 pA, $n = 5$). This result indicates that the decrease in the ratio of AMPAR- to NMDAR-mediated EPSCs was indeed, at least in part, caused by a decrease in the relative contribution of AMPARs to the synaptic currents. Furthermore, consistent with the immunocytochemical data, a significant decrease in mEPSC frequency was observed in the picrotoxin-treated cultures (6.2 ± 1.1 Hz in control cultures; 2.0 ± 0.6 Hz in picrotoxin-treated cultures). However, given the decrease in mEPSC amplitude, this observed decrease in mEPSC frequency must be interpreted cautiously. As was the case for Flag-GluR1, Western blotting revealed that the picrotoxin treatment had no detectable effect on the level of expression of endogenous GluR1 or GluR2/3 (not shown).

DISCUSSION

We have demonstrated that neural activity can differentially regulate the surface expression of subtypes of glutamate receptors at individual synapses. Specifically we found that the increase in activity induced by blockade of inhibitory synaptic transmission in networks of cultured hippocampal neurons caused a decrease in the percentage of synapses that contained the exogenously expressed AMPAR subunit Flag-GluR1 in their postsynaptic membranes. In contrast, this manipulation had no effect on the surface expression of the NMDAR subunit HA-NR1. This decrease in the synaptic targeting of GluR1 was dependent on activation of NMDARs, suggesting that the activity-dependent regulation of AMPAR targeting to synaptic membranes may play a role in NMDAR-dependent events such as synaptic plasticity. From the immunocytochemical data, we cannot establish that the epitope-tagged receptors were incorporated with endogenous subunits into normal heteromeric AMPARs or NMDARs. However, the electrophysiological data strongly suggest that the phenomenon we

observed also occurs with endogenous receptors and has clear functional consequences.

Previous work has found that blockade of activity during synaptogenesis in cultured spinal cord neurons does not affect the subcellular redistribution of AMPARs from a diffuse pattern to punctate synaptic clustering (15). However, NMDARs did not appear to contribute to synaptic currents in this system (19). Consistent with our hypothesis that activity can differentially regulate AMPAR and NMDAR clustering at synapses is the recent finding that chronic blockade of activity in cultured hippocampal neurons alters the subcellular distribution of NMDARs at synapses without affecting the distribution of AMPARs (20). This study, however, did not distinguish surface receptors from cytoplasmic pools (15, 20), and measurements of synaptic currents were not made. Data presented here show directly that activity causes changes in the clustering of AMPARs in the synaptic plasma membrane and, as a consequence, that a significant change in synaptic function occurs. Such a mechanism likely contributes to the decrease in the amplitude of mEPSCs that was observed after chronic blockade of inhibition in cortical cultures (21).

The protracted time course of the activity-dependent decrease in surface AMPAR synaptic clusters, which took between 2 and 7 days to reach its maximum extent, raises several interesting mechanistic questions. Given the relatively long half-life of surface AMPARs, which is estimated to be about 30 hr (15), this time course may reflect the activity-dependent generation of a signal that prevented the insertion of new AMPARs. Such a mechanism might account for the large proportion of silent synapses that have been suggested to exist early in development in a number of different neural circuits (8–10). Another possibility is that activity regulates the rate of removal of AMPARs from the synaptic plasma membrane. It is interesting to note that a very modest level of spontaneous activity was observed when recordings were made from individual neurons and that addition of picrotoxin induced relatively low frequency (0.1–2 per min), prolonged (>1 sec) bursts of activity that remained for the duration of the recording (>20 min) (*n* = 3). It is therefore possible that more robust increases in activity would generate a more rapid internalization of Flag-GluR1, analogous to the rapid internalization of G protein-coupled receptors that occurs in response to ligand activation (22, 23). If activity can control the internalization of AMPARs, such a mechanism could contribute to the expression of NMDAR-dependent long-term depression.

The ability to express recombinant GluR subunits in hippocampal neurons should greatly facilitate the elucidation of the molecular mechanisms responsible for the activity-dependent regulation of AMPAR and NMDAR targeting to synapses and synaptic membranes. It is well established that the C termini of NMDAR, but not AMPAR, subunits interact with PSD-95 (24) whereas the C terminus of some AMPAR subunits interact with the synaptic protein GRIP (25). Interference with the AMPAR/GRIP interaction disrupts the clustering of AMPARs at the synapse (25). Thus these subtype-specific molecular interactions are prime candidates for playing important roles in the effects observed here. Additional important issues for future work include elucidating the NMDAR-dependent signal transduction cascade that is re-

sponsible for the decrease in the surface expression of AMPAR clusters at synapses and determining under what conditions these changes occur *in vivo*.

1. Nakanishi, S. (1992) *Science* **258,** 597–603.
2. Seeburg, P. H. (1993) *Trends Neurosci.* **16,** 359–365.
3. Hollmann, M. & Heinemann, S. (1994) *Annu. Rev. Neurosci.* **17,** 31–108.
4. Bekkers, J. M. & Stevens, C. F. (1989) *Nature (London)* **341,** 230–233.
5. Sheng, M. (1997) *Nature (London)* **386,** 221–223.
6. Isaac, J. T. R., Nicoll, R. A. & Malenka, R. C. (1995) *Neuron* **15,** 427–434.
7. Liao, D., Hessler, N. A. & Malinow, R. (1995) *Nature (London)* **375,** 400–404.
8. Durand, G. M., Kovalchuk, Y. & Konnerth, A. (1996) *Nature (London)* **381,** 71–75.
9. Wu, G., Malinow, R. & Cline, H. T. (1996) *Science* **274,** 972–976.
10. Isaac, J. T. R., Crair, M. C., Nicoll, R. A. & Malenka, R. C. (1997) *Neuron* **18,** 269–280.
11. Kullmann, D. M. & Asztely, A. (1998) *Trends Neurosci.* **21,** 8–14.
12. Hampson, D. R., Huang, X. P., Oberdorfer, M. D., Goh, J. W., Auyeung, A. & Wenthold, R. J. (1992) *Neuroscience* **50,** 11–22.
13. Eshhar, N., Petralia, R. S., Winters, C. A., Niedzielski, A. S. & Wenthold, R. J. (1993) *Neuroscience* **57,** 943–964.
14. Richmond, S. A., Irving, A. J., Molnar, E., McIlhinney, A. J., Michelangeli, F., Henley, J. M. & Collingridge, G. L. (1996) *Neuroscience* **75,** 69–82.
15. Mammen, A. L., Huganir, R. L. & O'Brien, R. J. (1997) *J. Neurosci.* **17,** 7351–7358.
16. Lester, R. A. J., Quarum, M. L., Parker, J. D., Weber, E. & Jahr, C. E. (1989) *Mol. Pharmacol.* **35,** 565–570.
17. Brewer, G. J., Torricelli, J. R., Evege, E. K. & Price, P. J. (1993) *J. Neurosci. Res.* **35,** 567–576.
18. Hardy, S., Kitamura, M., Harris-Stansil, T., Dai, Y. & Phipps, M. L. (1997) *J. Virol.* **71,** 1842–1849.
19. O'Brien, R. J., Mammen, A. L., Blackshaw, S., Ehlers, M. D., Rothstein, J. D. & Huganir, R. L. (1997) *J. Neurosci.* **17,** 7339–7350.
20. Rao, A. & Craig, A. M. (1997) *Neuron* **19,** 801–812.
21. Turrigiano, G. G., Leslie, K. R., Desai, N. S., Rutherford, L. C. & Nelson, S. B. (1998) *Nature (London)* **391,** 892–896.
22. von Zastrow, M. & Kobilka, B. K. (1992) *J. Biol. Chem.* **267,** 3530–3538.
23. von Zastrow, M., Link, R., Daunt, D., Barsh, G. & Kobilka, B. (1993) *J. Biol. Chem.* **268,** 763–766.
24. Kornau, H.-C., Schenker, L. T., Kennedy, M. B. & Seeburg, P. H. (1995) *Science* **269,** 1737–1740.
25. Dong, H., O'Brien, R. J., Fung, E. T., Lanahan, A. A., Worley, P. F. & Huganir, R. L. (1997) *Nature (London)* **386,** 279–284.